

Effect Investigation of Zn Substitution on the characterization of Cobalt Ferrite Nano Particles Prepared Co-precipitation method

¹Ahmed Saied Faheim El-Saaey, ²Abd El Fattah Mustafa Khourshid, ³Alaa-ELdin A. EL-Hammady, ⁴Abdul Rahman Abdullah Badawi

¹Mechanical & electrical research institute, National water research Centre, Egypt

²Mechanical Design Department, Faculty of Engineering, Tanta University

³Mechanical Design Department, Faculty of Engineering, Tanta University

⁴physical chemistry National Research Center, Doke, Cairo, Egypt

Abstract: Nano-crystalline zinc-substituted cobalt ferrite powders, $Co_{1-x}Zn_xFe_2O_4$ ($x=0.0, 0.1, 0.3, 0.5, 0.7, 0.9$ and 1.0), have been synthesized by the Co-precipitation method. The structural and magnetic properties of the products were determined and characterized in detail by X-ray diffraction (XRD), High Resolution-Transmission Electron Microscope (HR-TEM), Fourier Transform Infrared (FTIR) and vibrating sample magnetometer (VSM). X-ray analysis showed that the samples were cubic spinel. The increase in zinc concentration resulted in an increase in the lattice constant, X-ray density, ionic radii, the distance between the magnetic ions and bond lengths on tetrahedral sites and octahedral sites of cubic spinel structure. The HR-TEM and XRD shows that crystallite size within the range of 6–24 nm. The FTIR measurements between 400 and 2000 cm^{-1} confirmed the intrinsic cation vibrations of the spinel structure. The variation of saturation magnetization (M_s) value of the samples was studied and magnetic coercivity. The magnetic measurements show that the saturation magnetization and coercivity decrease by increasing the zinc content. Furthermore, the results reveal that the sample with a chemical composition of $Co_{0.3}Zn_{0.7}Fe_2O_4$ exhibits the super-paramagnetic behavior.

Keywords: Nano size, Co-precipitation method, $Co_{1-x}Zn_xFe_2O_4$, XRD, TEM, VSM, FTIR.

I. Introduction:

Nanoparticles of complex metal oxides such as spinel ferrites are thermally and chemically stable. The nanoparticles possess great potentials for application in catalysis, gas sensors, high quality ceramics and super paramagnetic materials [1–2]. The properties of these materials mainly depend on their shape, size, and structure, which are strongly determined by the synthetic processes [3–2]. There are several different synthesis methods used to fabricate ferrites as reviewed in the literature including sol-gel, combustion methods, hydrothermal, mechano-chemical, refluxing and co-precipitation method [4–5, 6–7].

The magnetic property can be altered by the addition of zinc. Addition of zinc also affects the lattice parameter (a_0). Various preparation techniques, such as reverse micelle technique [8–9], sol-gel pyrolysis method [10] hydrothermal technique [11] and mechanical alloying [12] are used to prepare ferrite nanoparticles. But co-precipitation method is considered to be economical means of producing fine particles [13, 14]. The electrical and dielectrical properties were also studied for Co-Zn ferrite, it was reported that the composition $Co_{0.6}Zn_{0.4}Fe_2O_4$ has a high value of electrical conductivity, dielectric constant and magnetic permeability [15, 16].

Therefore, in this work we structural and magnetic properties of nano-crystalline cobalt zinc ferrite in relation to the concentration of zinc, which are three metal element systems, prepared by Co-precipitation method.

II. Experimental:

2.1 Materials:

All chemical re-agents—ferric chloride $FeCl_3$, cobalt(II) chloride $CoCl_2$, zinc(II) chloride $ZnCl_2$ and sodium hydroxide $NaOH$ —were purchased from (El-Gomhouria Co. for Drugs), Egypt and used as received without further treatment.

2.2 Instrumentation:

X-ray powder diffraction analysis was conducted on a Bruker Axs-D8 Advance Diffractometer (XRD).

FTIR transmission spectra were taken on Perkin Elmer Spectrum BX model Infrared Spectrophotometer from 2000 to 400 cm^{-1} .

High Resolution-Transmission Electron Microscopy (HR-TEM) analysis was performed on (JEOL 2000FX).

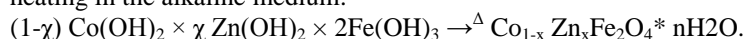
Magnetic measurements were carried out with the Quantum Design Model 6000 Vibrating Sample Magnetometer (VSM) and parameters like specific saturation magnetization (Ms), coercive force (Hc) and remanence (Mr) were evaluated.

2.3 Procedures:

The magnetization of substituted ferrite nanoparticles synthesized by co-precipitation depends mostly on parameters such as reaction temperature, pH of the suspension, initial molar concentration etc. [17]. Ultra-fine particles of $(Co_{1-x}Zn_x)Fe_2O_4$ with $x = 0.0, 0.1, 0.3, 0.5, 0.7, 0.9$ and 1 . The defined from A1, A2, A3, A4, A5, A6 and A7 respectively) were prepared by co-precipitating aqueous solutions of $CoCl_2, ZnCl_2$ and $FeCl_3$ mixtures, respectively, in alkaline medium. The mixed solution of $CoCl_2, ZnCl_2$ and $FeCl_3$ in their respective stoichiometry (100 ml of 0.1 M $CoCl_2$, 100 ml of 0.9 M $ZnCl_2$ and 100 ml of 2 M $FeCl_3$ in the case of $Co_{0.1}Zn_{0.9}Fe_2O_4$ and similarly for the other values of x) was prepared and kept at 60 °C. This mixture was added to the boiling solution of NaOH (1 M dissolved in 1200 ml of distilled water) within 10 s under constant stirring. Nanoferrites are formed by conversion of metal salts into hydroxides, which take place immediately, followed by transformation of hydroxides into ferrites. At first solid hydroxides of metals in the form of fine particles were obtained by the co-precipitation of metal cations in alkaline medium (co-precipitation step):



The solid solution of metal hydroxides was transformed to complex zinc substituted ferrites when subjected to heating in the alkaline medium:



The solutions were maintained at 80 °C for 2 h. This duration was sufficient for the transformation of hydroxides into spinel ferrite (dehydration and atomic rearrangement involved in the conversion of intermediate hydroxide phase into ferrite) [17]. Sufficient amount of fine particles were collected at this stage by using magnetic separation. These particles were washed several times with distilled water and dried at 100 °C temperature.

III. Results and Discussions:

3.1. Physical characterization:

The X-ray diffraction patterns (fig 1) of the prepared samples, $Co_{1-x}Zn_xFe_2O_4$ (with $x = 0.0, 0.1, 0.3, 0.5, 0.7, 0.9$ and 1.0) exhibited.

The (6) reflection planes (2 2 0), (3 1 1), (4 0 0), (4 4 2), (5 1 1), and (4 4 0), that indicate the presence of the spinel cubic structure [18].

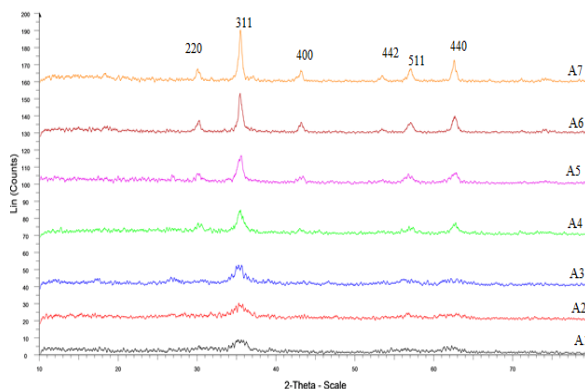


Fig. (1)

The nature of the peak changes by the change in composition. The absence of extra peaks than due to the spinel phase of ferrite, indicates that all the compositions contain only a single phase of spinel structure. The patterns indicate well-defined peaks of crystalline FCC phase which confirm spinel cubic structure formation. No additional impurity reflections due to phase purity. The crystallite size of the studied samples calculated using Debye-Scherrer formula is shown in (fig. 2, 3) and shows the variation of crystal size and lattice constant with Zn content in the ferrites. The zinc substitution process brought about different modifications in the structural properties such as lattice constant, unit cell volume, ionic radii, the distance between the magnetic ions and bond lengths on tetrahedral sites and octahedral sites of cubic spinel structure for the produced cobalt ferrite crystallites. These properties of Co-Zn ferrite increase as the concentration of zinc increases. These findings could be attributed to the higher ionic radius of zinc than that of cobalt species [19].

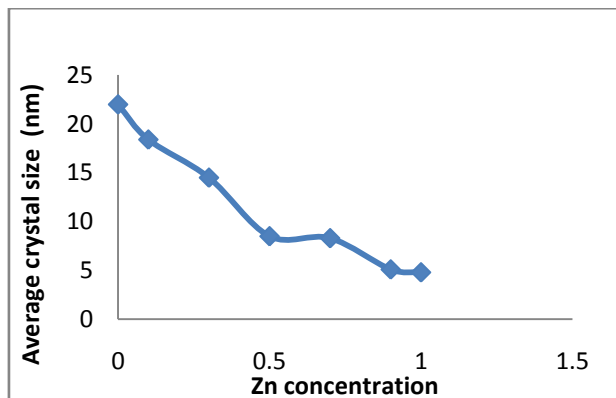


Fig. (2)

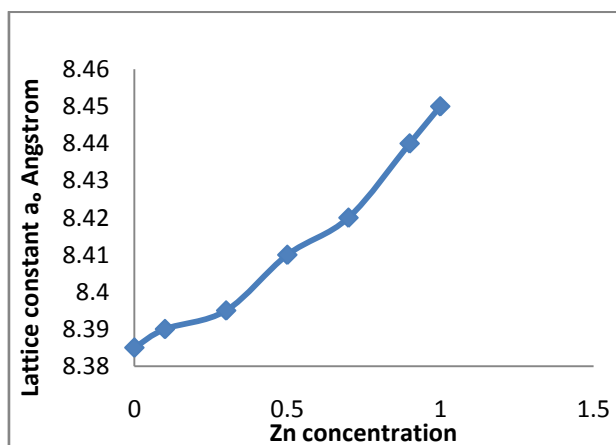


Fig. (3)

Furthermore, substitution of Zn ions will cause migration of Fe^{3+} from A-site to B-site causing an overall change of the lattice. The increase in intensity of (220) and (422) reflections by increasing Zn content reveals that Zn ions occupy A-site, therefore the spinel structure transfer gradually to inverse spinel structure by increasing Zn. The shifts in peak positions are due to the substitution of Zn in $CoFe_2O_4$ lattice and the subsequent formation of Zn Co ferrite nanoparticles. The XRD patterns also show a slight shift in peaks position towards higher d-spacing values with increasing Zn content in the ferrite. Therefore the Co Zn ferrite system has unit cell consisting of eight formula units of the form $[Zn_x^{2+} Fe_{1-x}^{3+}]_A [Co_{1-x}^{2+} Fe_{1+x}^{3+}]_B O_4^{2-}$. The Zn^{2+} ions have preference for tetrahedral site whereas Co for octahedral site. [20, 21].

3.2 Transmission Electron Microscope (TEM) measurement and Analysis:

Prepared samples were characterization by TEM as shown in Fig (4) to fig (10). Analysis of TEM measurements shows that average particle size is nearly 24nm.

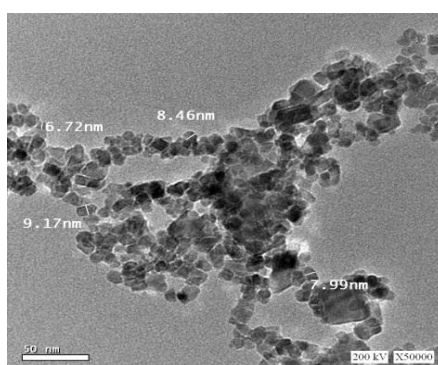


Fig. (4). TEM images of A1

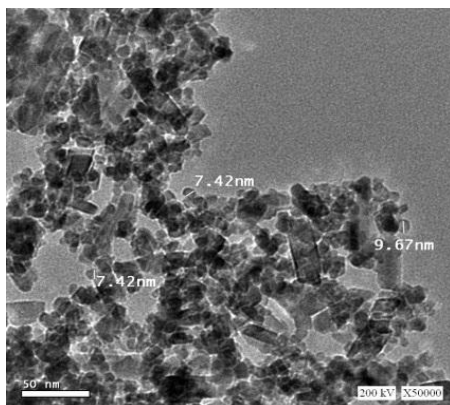


Fig. (5).TEM images of A2

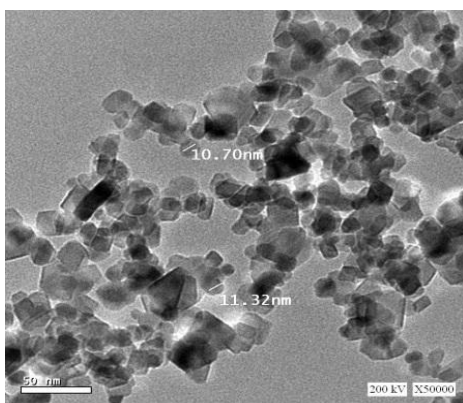


Fig. (6).TEM images of A3

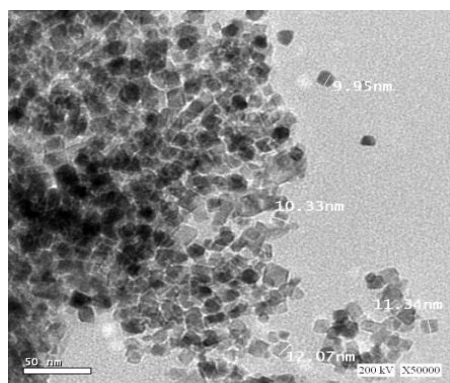


Fig. (7).TEM images of A4

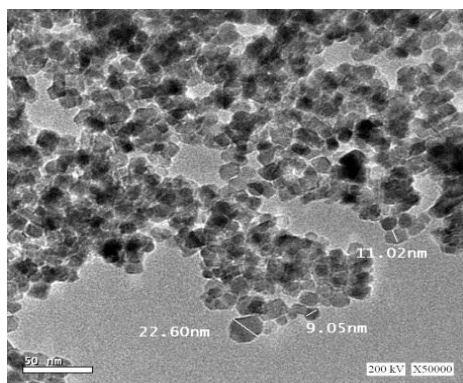


Fig. (8).TEM images of A5

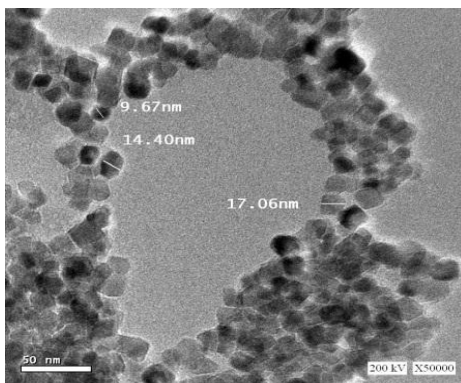


Fig. (9).TEM images of A6

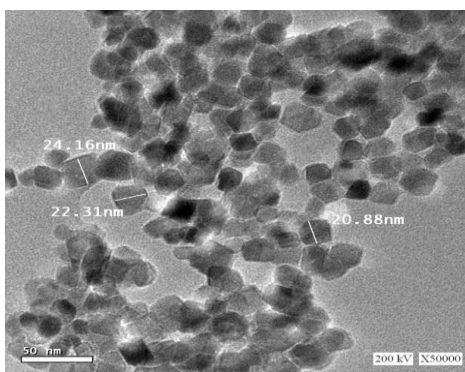


Fig. (10).TEM images of A7

3.3 FTIR analysis:

In the FT-IR spectra the frequency bands near $564\text{--}588\text{ cm}^{-1}$ and $425\text{--}442\text{ cm}^{-1}$ are assigned to the tetrahedral and octahedral clusters and confirms the presence of M-O stretching band in ferrites as suggested by Pradeep and Chandrasekaran [22]. The authors suggested that the vibrational mode of tetrahedral clusters is higher as compared to that of octahedral clusters, which is attributed to the shorter bond length of tetrahedral clusters.

So, FT-IR not only used to collect information about the structure of a compound, but it is also utilized as an analytical tool for assessing the purity of a compound. Fig. 6 exhibits the FTIR absorption bands for various zinc concentration spinel ferrites at room temperature in the wave number range of $400\text{--}2000\text{ cm}^{-1}$. It is obvious that the higher frequency band (U_1) around 600 cm^{-1} and the lower frequency band (U_2) is around 400 cm^{-1} shows that in fig (11).

The highest one corresponds to the intrinsic stretching vibrations of the metal at the tetrahedral site, whereas the U_2 -lowest band is assigned to octahedral-metal stretching [23, 24].

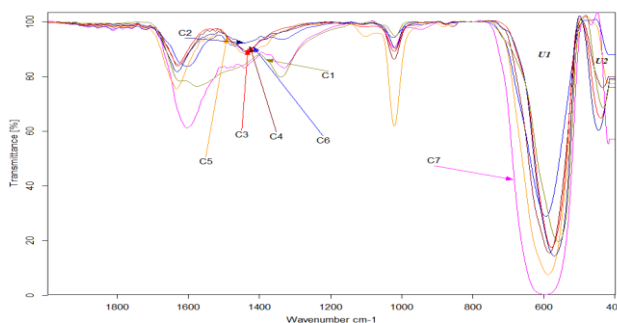


Fig.(11)

3.4. Magnetic properties:

3.4.1. Saturation magnetization

Fig. (12,13,14) Shows that as the zinc content increases, the saturation magnetization and coercivity decrease and lead to the superparamagnetic behavior [25]. Also this figure exhibits the low field onset of

A3 sample for better visualization of magnetic coercivity. The reduction in magnetization from 38.443 to 2.237 Am²/kg (Table 2) can be expressed as follows:

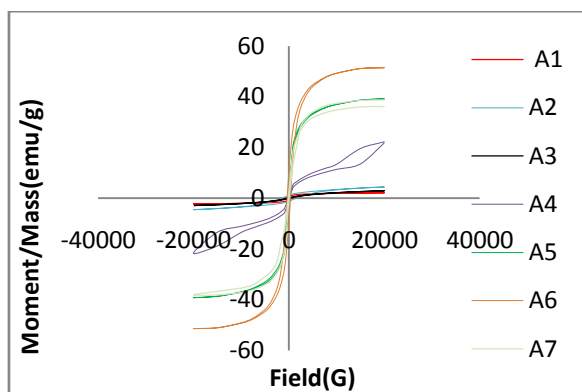


Fig. (12)

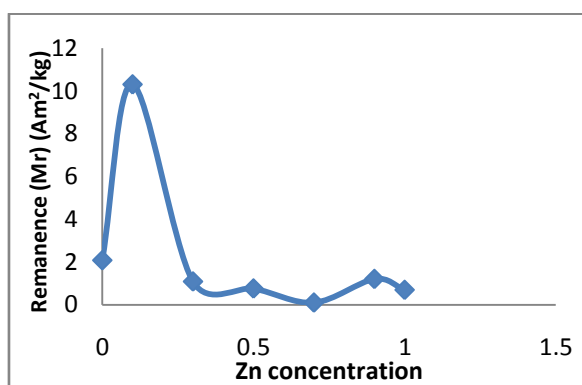


Fig (13)

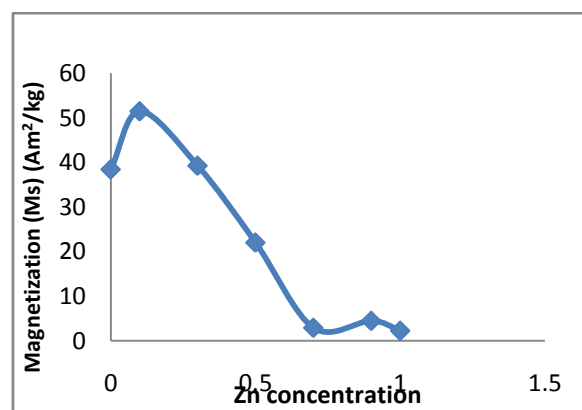


Fig (14)

a) **Weakening of A–B interactions:** as zinc replaces some of the Co ions, the magnetic coupling weakens because zinc itself does not carry the magnetic moment. The mechanism of the substitution can be described by replacing cobalt cations by non-magnetic zinc cations $[Zn_x^{2+} Fe_{1-x}^{3+}]_A [Co_{1-x}^{2+} Fe_{1+x}^{3+}]_B O_4^{2-}$ which prefer the tetrahedral sites. At high concentrations of Zn²⁺ approximately for (X > 0.5), it leads to the weakening of the A–B interactions and thus leads to a disturbance of the spin ordering, causing the destabilization of the magnetic ordering.

b) **Size reduction:** as the zinc concentration increases, the particles size and the degree of crystallinity decrease. The existence of some degree of the spin canting in the whole volume of the nanoparticles and the disordered surface/dead layer at the surface can explain the decrease of the saturation magnetization [26].

In other words, at Zn concentration (0.7) the particles become super-paramagnetic, the powders cannot be saturated easily and the magnetic moments within a particle rotate easily with temperature [25]. Additionally,

the lack of oxygen to mediate the super-exchange mechanism between the nearest iron ions on the surface can lead to a decrease in the exchange couple, resulting in slanted spins and a decrease in the nanoparticle saturation magnetization. This can also be attributed to the enhancement of the surface barrier potential due to the distortion of the crystal lattice caused by the atoms deviating from the normal positions in the surface layers [27–28].

Sample	Ms(emu/g)	Mr(emu/g)	Mr/Ms	Hc(Am ² /kg)
A1	2.237	0.69356	0.31004	56.211
A2	4.4468	1.2045	0.27086	120.989
A3	2.8989	9.92E-02	0.0034	1.6225
A4	22.01	0.75759	0.0344	10.8328
A5	39.267	1.0852	0.0276	3.6432
A6	51.481	10.302	0.2001	27.1995
A7	38.443	2.0775	0.0540	9.7378

Table (1). Magnetic parameters

3.5.2. Magnetic coercivity

The reduction in magnetic coercivity with the Zn content from 120 to 1.6 Am²/kg show in fig(15) can be described as follows:

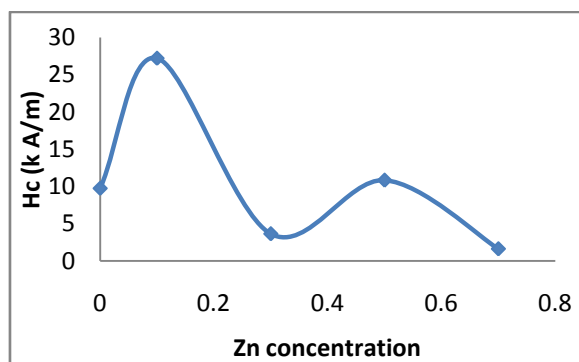


Fig (15).

a) **Size effect:** as the particle size decreases below a critical size or magnetic exchange length, L_{ex} , H_C follows a D^6 power law {Eq. (1)}[29], where A is the exchange stiffness constant, and P_C is a constant of the order of unity. L_{ex} can be expressed as $L_{ex} = \sqrt{\frac{A}{K_1}}$. The critical size of Co–ferrites for the single domain behavior, depending on composition, is between 30 and 70 nm[30]. That is, for $D \gg D_{crit}$, one would expect H_C to decrease by increasing the crystallite size as the system enters the multi-domain region.

$$H_c = \frac{P_c K_1^4 D^6}{\mu_0 M_s A^4} \quad (1)$$

b) **Magneto-crystalline anisotropy:** the large coercivity in bulk stoichiometric $CoFe_2O_4$ has traditionally been explained by the single-ion anisotropy model, arising from the contribution of the orbital magnetism of Co^{2+} ions at the [B] sites ($CoFe_2O_4$, high-spin Co^{2+} ions). That is, when the Co^{2+} ions migrate from the octahedral sites to the tetrahedral ones because of the variations in the inversion, the coercivity decreases due to the less anisotropic environment of the tetrahedral sites. $CoFe_2O_4$ is only weakly anisotropic at room temperature because of the presence of low-spin Co^{2+} ions [31].

In addition to the Co migration, another reason is the angular momentum of the zinc ion. Zn^{2+} has a zero angular momentum ($l=0$) and does not contribute to magneto-crystalline anisotropy. As the zinc ion ($l=0$) replaces some of the Co ions ($d^7, l \neq 0$), the spin–orbit coupling weakens because zinc itself does not carry the angular momentum; consequently, the magnetic anisotropy and magnetic coercivity will decrease {Eq. (2)}. Another possible factor influencing the magnetic properties would be the stress anisotropy due to the large magnetostriction of $CoFe_2O_4$ ($\lambda_s = -260 \times 10^{-6}$) because different particles exhibit diverse micro-strain values. By increasing the Zn content the magnetostriction coefficient of ferrite will decrease. In this equation the K_1 is the magnetic anisotropy and M_s is the saturation magnetization.

$$H_c = \frac{2K_1}{M_s} \quad (2)$$

IV. Conclusions:

Using chloride of nickel, cobalt, and iron in combination with sodium hydroxide, fine cobalt doped zinc ferrite powders have been successfully synthesized Co-precipitation method. This suggests that this method is suitable not only to synthesize two metal systems but also systems containing three metals and economical chemical co-precipitation method. The Co-ferrite, which is a kind of inverse spinel oxide, and belongs to a square group $O_h^7(Fd3m)$, has been widely investigated because of its cubic magneto-crystalline anisotropy, relatively high coercivity, moderate saturation magnetization and good chemical stability. Also, the microstructural and magnetic properties were discussed in detail:

1. The XRD patterns revealed that the spinel cubic structure is formed for the synthesized materials.
2. The growth of particles is obstructed by the presence of zinc so that the average particle size decreases from 24 nm to 6 nm as the concentration of zinc is increased from X=0 to X=1. A possible reason may be the difference in the formation of the enthalpy of $ZnFe_2O_4$ and $CoFe_2O_4$, which modifies the growth conditions. It may also have some relation to the fact that all the cation preferences are not satisfied when Zn is introduced in the Co-Zn ferrite.
3. By increasing the zinc content the lattice parameter is decreased as a result of the high ionic radius of Zn^{2+} and the decrease in grain size.
4. As the zinc content increases the saturation magnetization, the coercivity decreased and the best composition is about $Zn=0.7$.

Acknowledgement

This work was financial supported by National Water Research Center (NWRC).

References

- [1]. B.P. Barbero, J.A. Gamboa, L.E. Cadus, Appl. Catal.B 65 (2006) 21.
- [2]. L.J. Zhao, H.J. Zhang, Y. Xing, S.Y. Song, S.Y. Yu, W.D. Shi, X.M. Guo, J.H. Yang, Y.Q. Lei, F. Cao, J. Solid State Chem. 181 (2008) 245.
- [3]. N.M. Deraz, J. Anal.Appl.Pyrol.82 (2008) 212.
- [4]. N.M. Deraz, S. Shaban, J. Anal.Appl.Pyrol.86 (2009) 173
- [5]. S. Ayyappan, J. Philip, B. Raj, Mater. Chem.Phys.115 (2009) 712
- [6]. A. Pradeep, P. Priyadharsini, G. Chandrasekaran, J. Magn.Magn.Mater. 320 (2008) 2774.
- [7]. X.D. Li, W.S. Yang, F. Li, D.G. Evans, X. Duan, J. Phys.Chem.Solids 67 (2006) 1286
- [8]. A. Kale, S. Gubbala, R.D.K. Misra, J. Magn. Magn.Mater.277 (2004) 350.
- [9]. S. Gubbala, H. Nathani, K. Koizol, R.D.K. Misra, Physica B 348 (2004) 317.
- [10]. J.-G. Lee, H. Minlee, C.S. Kim, J. Magn. Magn.Mater. 900 (1998)177.
- [11]. K.J. Davis, K.O. Grady, S. Morup, J. Magn. Magn.Mater.149 (1995) 14.
- [12]. J. Ding, P.G. McCormick, R. Street, J. Magn.Magn.Mater.171 (1997) 309.
- [13]. R.V. Upadhyay, R.V. Metha, K. Parekh, D. Srinivas, R.P. Pant, J. Magn. Magn.Mater.201 (1999) 129.
- [14]. Y. Shi, J. Ding, X. Liu, J. Wang, J. Magn. Magn.Mater. 205 (1999) 249..
- [15]. M.A. Ahmed, M.K. El-Nimr, A. Tawfik, A.M. Abbo El-Ata, J. Mater. Sci. Lett. 7(1988) 639.
- [16]. B.K. Kuanr, G.P. Srivatava, J. Appl. Phys. 75 (1994) 6115.
- [17]. B. Jeyadevan, C.N. Chinnasamy, K. Shinoda, K.Tojji, J. Appl.Phys. 93 (2003) 8450.
- [18]. A.M. El Sayed, Ceram. Int. 28 (2002) 363.
- [19]. V.G. Patil, S.E. Shirsath, S.D. More, S.J. Shukla, K.M. Jadhav, J. Alloys Compd. 488 (2009) 199
- [20]. N.M. Deraz, J. Anal.Appl.Pyrol.88 (2010) 103.
- [21]. N.M. Deraz, A. Alarifi, Polyhedron 28 (2009) 4122.
- [22]. A. Pradeep and G. Chandrasekaran, "FTIR Study of Ni, Cu and Zn Substituted Nanoparticles of $MgFe_2O_4$," Material Letters, Vol. 60, No. 3, 2006, pp. 371-374.
- [23]. Y. Koseoglu, M. Bay, M. Tan, A. Baykal, H. Sozeri, R. Topkaya, N. Akdogan, Magnetic and dielectric properties of $Mn_{0.2}Ni_{0.8}Fe_2O_4$ nanoparticles synthesized by PEG-assisted hydrothermal method, Journal of Nanoparticle Research 13 (2010) 2235–2244.
- [24]. R.D.D. Waldron, Infrared Spectra of Ferrite, Physical Review 99 (1955) 1727–1735.
- [25]. D.S. Mathew, R.-S. Juang, An overview of the structure and magnetism of spinel ferrite nanoparticles and their synthesis in microemulsions, Chemical Engineering Journal 129 (2007) 51–65.
- [26]. E. Pollert, P. Veverka, M. Veverka, O. Kaman, K. Zveta, S. Vasseur, R. Epherre, G. Goglio, E. Duguet, K. Zaveta, Search of new core materials for magnetic fluid hyperthermia: preliminary chemical and physical issues, Progress in Solid State Chemistry 37 (2009) 1–14.
- [27]. H.Y. He, Comparison study on magnetic property of $Co_{0.5}Zn_{0.5}Fe_2O_4$ powders by template-assisted sol-gel and hydrothermal methods, Journal of Materials Science: Materials in Electronics (2011) 1–6. DOI:(10.1007/s10854-011-0535-2).
- [28]. A.E. Berkowitz, W.J. Schuele, Magnetic properties of some ferrite micropowders, Journal of Applied Physics 30 (1959). S134–S134.
- [29]. Q. Zeng, I. Baker, V. McCreary, Z. Yan, Soft ferromagnetism in nanostructured mechanical alloying FeCo-based powders, Journal of Magnetism and Magnetic Materials 318 (2007) 28–38.
- [30]. A.E. Berkowitz, W.J. Schuele, Magnetic properties of some ferrite micropowders, Journal of Applied Physics 30 (1959). S134–S134
- [31]. G. Salazar-Alvarez, R.T. Olsson, J. Sort, W.A.A. Macedo, J.D. Ardisson, M.D. Baro', U.W. Gedde, J. Nogues, Enhanced coercivity in Co-rich near stoichiometric $CoxFe_{3-x}O_4$ nanoparticles prepared in large batches, Chemistry of Materials 19 (2007) 4957–4963.